scattering electrons – mostly due to single or multiple elastic events – and of an important fraction of inelastic electrons suffering more than one energy loss. The probability of having n inelastic processes of mean free path Λ is governed by the Poisson distribution:

$$P_n(t) = \frac{1}{n!}\left(\frac{t}{\Lambda}\right)^{-n} \exp\left(-\frac{t}{\Lambda}\right). \qquad (4.3.4.6)$$

Multiple losses introduce additional peaks in the energy-loss spectrum; they are also responsible for an increased background that complicates the detection of single characteristic core-loss signals. Consequently, when the specimen thickness is not very small (*i.e.* for $t \gtrsim 50$ nm for 100 keV primary electrons), it is necessary to retrieve the single scattering profile that is truly representative of the electronic and chemical properties of the specimen.

Deconvolution techniques have therefore been developed to remove the effects of plural scattering from the low-loss spectrum (up to 100 eV) or from ionization edges but very few treatments deal with both angle and energy-loss distributions. Batson & Silcox (1983) have made a detailed study of the inelastic scattering properties of incident 75 keV electrons through a ~100 nm thick polycrystalline aluminium film, over the full range of transferred wavevectors ($0 \rightarrow 3$ Å^{-1}) and energy losses ($0 \rightarrow 100$ eV). Schattschneider (1983) has proposed a matrix approach that is sufficiently elaborate to handle angle-resolved energy-loss data. Simpler deconvolution schemes have been proposed and used for processing multiple losses without specific consideration of angular truncation effects. They are valid when the data have been recorded over sufficiently large angles of collection so that all appreciable inelastic scattering is included. They are generally based on Fourier transform techniques, except for the iterative approach of Daniels, Festenberg, Raether & Zeppenfeld (1970), which has been used for energy losses up to about 60 eV (Colliex, Gasgnier & Trebbia, 1976). The most accurate current methods are the Fourier-log method of Johnson & Spence (1974) and Spence (1979), and the Fourier-ratio method of Swyt & Leapman (1982), which only applies to the core-loss region. The first is far more complete and accurate and applies to any spectral range when one has recorded a full spectrum in unsaturated conditions.

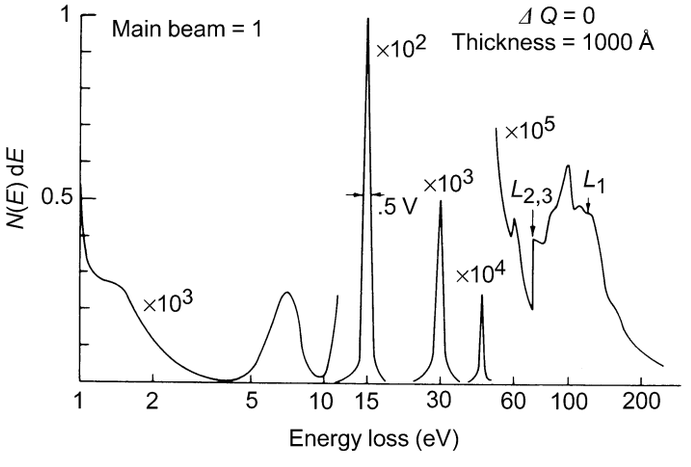

Fig. 4.3.4.3. Excitation spectrum of aluminium from 1 to 250 eV, investigated by EELS on 300 keV primary electrons [courtesy of Schnatterly (1979)].

4.3.4.1.4. *Classification of the different types of excitations contained in an electron energy-loss spectrum*

Figs. 4.3.4.3 and 4.3.4.4 display examples of electron energy-loss spectra over large energy domains, typically from 1 to about 2000 eV. With one instrument, all elementary excitations from the near infrared to the X-ray domain can be investigated. Apart from the main beam or zero-loss peak, two major families of electronic transitions can be distinguished in such spectra:

(*a*) The excitations in the low or moderate energy-loss region ($1 < \Delta E < 50$ eV) concern the quasifree (valence and conduction) electron gas. In a pure metal, such as Al, the dominant feature is the intense narrow peak at 15 eV with its multiple satellites at about 30, 45, and 60 eV. One also detects an interband transition at 1.5 eV and a surface plasmon peak at ~ 7 eV. For the more complex mineral specimen, rhodizite, this contribution lies in the intense and broad, but not very specific, peak around 25 eV. All these features are discussed in detail in Subsection 4.3.4.3.

(*b*) The excitations in the high-energy-loss domain ($50 < \Delta E < 2000$ eV) concern excitation and ionization processes from core atomic orbitals: in Al, the $L_{2,3}$ edge is associated with the creation of holes on the $2p$ level, L_1 is due to the excitation of $2s$, and K of $1s$ electrons. These contributions appear as edges superposed on a regularly decreasing background. In the complex specimen, the succession of these

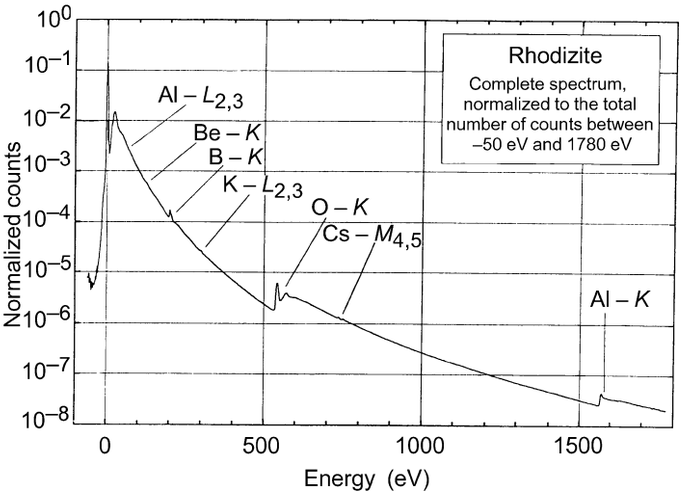

Fig. 4.3.4.4. Complete electron energy-loss spectrum of a thin rhodizite crystal (thickness ~60 nm). Separate spectra from eight significantly overlapping energy ranges were measured and matched. Primary energy 60 keV. Semi-angle of collection 5 mrad. Recording time 300 s (parallel acquisition). Scanned area 30×40 nm. Analysed mass 2×10^{-15} g [courtesy of Engel, Sauer, Zeitler, Brydson, Williams & Thomas (1988)].

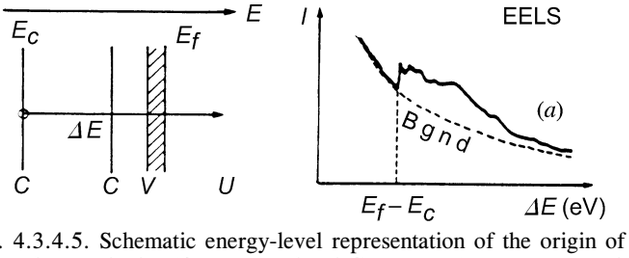

Fig. 4.3.4.5. Schematic energy-level representation of the origin of a core-loss excitation (from a core level C at energy E_c to an unoccupied state U above the Fermi level E_f) and its general shape in EELS, as superimposed on a continuously decreasing background.

references